Recibido: 03/08/2023
Aceptado: 16/01/2024

REVISTA DE TELEDETECCIÓN
Asociación Española de Teledetección
(2024) 63, 65-77
ISSN 1133-0953
EISSN 1988-8740
https://doi.org/10.4995/raet.2024.20158

Improving the evapotranspiration estimation by coupling soil moisture and atmospheric variables in the relative evapotranspiration parameterization

Elisabet Walker*[1,2], Virginia Venturini[1,2]

[1] *Facultad de Ingeniería y Ciencias Hídricas (FICH), Universidad Nacional del Litoral (UNL). Ciudad Universitaria, Ruta Nacional N°168 – km 472,4. Santa Fe (3000), Argentina.*

[2] *Consejo Nacional de Investigaciones Científicas y Técnicas (CONICET), Argentina.*

Abstract: Accurate monthly evapotranspiration (ET) estimation is essential for many forest, climate, and hydrological applications, as well as for some agricultural uses. In this study, the relationship between ET and relative evapotranspiration (F) using land surface, and atmospheric variables was assessed with 17 FLUXNET sites data in savanna, cropland, and forest land covers, distributed all over the world. A sigmoid (Fs) and a logarithmic (Fl) F expression were included in Walker *et al.*'s (2019a,b) equations to evaluate their impact on the accuracy of ET estimations. The new parameterizations of ET outperformed the original expression, showing root mean square errors lower than 24% of the mean observed ET. The results presented here suggest that atmospheric parameters, coupled with land explanatory variables included in F estimates, produce more precise ET estimations. In addition, Soil Moisture Active Passive (SMAP) products were used to obtain global maps of ET and compared with Global Land-surface Evaporation Amsterdam Methodology (GLEAM) and Terra Moderate Resolution Imaging Spectroradiometer (MODIS) MOD16 products, displaying the flexibility of these new parametrizations with different sources of data.

Key words: evapotranspiration, land covers, atmospheric variables, soil moisture, relative evapotranspiration.

Mejora en la estimación de la evapotranspiración mediante el acoplamiento de la humedad del suelo y variables atmosféricas en la parametrización de la evapotranspiración relativa

Resumen: La estimación precisa de la evapotranspiración (ET) mensual es esencial para muchas aplicaciones forestales, climáticas e hidrológicas y para algunos usos agrícolas. En este estudio, se evaluó la relación entre ET y la evapotranspiración relativa (F) utilizando variables de la superficie y atmosféricas con datos de 17 sitios FLUXNET en coberturas terrestres de sabana, cultivo y bosques, distribuidos por todo el mundo. Se incluyeron en las ecuaciones de Walker *et al.* (2019a,b) una expresión de F sigmoidea (Fs) y otra logarítmica (Fl) para evaluar su impacto en la precisión de las estimaciones de ET. Las nuevas parametrizaciones de ET superaron a la expresión original, mostrando errores cuadráticos medios inferiores al 24% de la ET media observada. Los resultados presentados aquí sugieren que los parámetros atmosféricos, junto con las variables explicativas de la superficie incluidas en las estimaciones de F, producen estimaciones de ET más precisas. Asimismo, los productos de *Soil Moisture Active Passive* (SMAP) fueron usados para obtener mapas globales de ET y comparados con los productos *Global Land-surface Evaporation Amsterdam Methodology* (GLEAM) y *Terra Moderate Resolution Imaging Spectroradiometer* (MODIS) MOD16, mostrando la flexibilidad de estas nuevas parametrizaciones con diferentes fuentes de datos.

Palabras clave: evapotranspiración, coberturas terrestres, variables atmosféricas, humedad del suelo, evapotranspiración relativa.

To cite this article: Walker, E., Venturini, V. 2024. Improving the evapotranspiration estimation by coupling soil moisture and atmospheric variables in the relative evapotranspiration parameterization. *Revista de Teledetección*, *63*, 65-77. https://doi.org/10.4995/raet.2024.20158

* *Corresponding author: ewalker@fich.unl.edu.ar*

1. Introducción

Actual evapotranspiration (ET) is a crucial process that represents surface-atmosphere interactions, a key component of the terrestrial water cycle that links the carbon cycle, and the energy balance. Monthly ET estimates with a long time series of data are required for applications such as vulnerable forests monitoring (wildfire), regional water balances, climate change studies, ecosystem evolution, and land cover changes impact on ET (Fisher *et al.* 2017; Liu *et al.* 2021; Poulos *et al.* 2021).

ET is a complex process to simulate given its dependence on many interacting processes controlling it. Three ET general driving forces were identified, *i.e.,* net radiation (Rn), atmospheric variables, and surface properties (Ma *et al.*, 2020; Zhou *et al.*, 2021). Thus, during the last decades, many efforts have been spent on studying the relationship between ET and these controlling factors to better estimate the ET process. The scientific community has proposed several models to estimate ET over a wide range of spatial and temporal scales, from remotely sensed information and ground observation networks (Allen *et al.*, 2001; Sun *et al.*, 2011; Walker *et al.*, 2019a,b; Brust *et al.*, 2021; Laipelt *et al.*, 2021; Yao *et al.*, 2023). Some of the abovementioned models have taken advantage of the complementary relationship (CR) to calculate ET. This relationship establishes a balance between ET, potential evapotranspiration (ETpot), and wet environmental evapotranspiration (ETw) (Brutsaert, 2015). The concept of ETw suggests that the surface temperature and wetness are unlimited while the energy available for evaporation is limited. The concept of ETpot represents an extreme situation, where there is no limitation for the ET process. Bouchet (1963) proposed the first complementary model based on an experimental design, for a wide range of available energy. In the attempt to derive a physically based CR, Granger (1989) assumed the inequality ETpot≥ETw≥ET, where ETw can be formulated using either Penman or Priestley–Taylor (P-T from here on) equations. Examples of successful ET models based on CR include those developed by Fisher *et al.* (2008), Venturini *et al.* (2008), Brutsaert (2015), Walker *et al.* (2019a,b), Ma *et al.* (2020), and Yunfei *et al.* (2023).

Walker *et al.*'s models (Walker *et al.*, 2019a,b), to estimate ET (named as ETsm and ETwv, respectively) were obtained by combining a CR, ETw calculated with P-T formulation, and the relative evapotranspiration (F) parameter, defined as the ratio between ET and ETpot. Indeed, Walker *et al.* (2019a) presented a mathematical F formulation based on Komatsu's expression (Komatsu, 2003) that considers the soil moisture content (SM), soil type properties and includes a calibration parameter X to avoid ET resistance coefficients estimation. Later, Walker *et al.* (2019b) presented an F formulation improving the relative evapotranspiration introduced by Venturini *et al.* (2008). As a result, the ratio between SM and the soil saturation water content (SMsat) replaced the original Venturini *et al.*'s (2008) F formulation in agreement with the ET-driven physical process.

It has been demonstrated that SM is a critical surface state variable on which ET depends (Purdy *et al.*, 2018; Zhou *et al.*, 2021; Yao *et al.*, 2023), and therefore had an important impact on ET/ETpot (Mintz and Walker, 1993; Komatsu, 2003; Detto *et al.*, 2006, Fisher *et al.,* 2008; Teng *et al.*, 2014; An *et al.*, 2018; Brust *et al.*, 2021). For example, Detto *et al.* (2006) analysed the F-SM relationship in a heterogeneous rain-fed Mediterranean ecosystem with three different land covers. Komatsu (2003), Teng *et al.* (2014), and later An *et al.* (2018), studied the effect of SM on F from bare soils data, acquired under controlled conditions. Fisher *et al.* (2008) proposed to constraint ET by a function of SM (fSM), which is an index of SM deficit based on the complementary hypothesis of Bouchet (1963). Their approach recognizes that evaporation is intrinsically driven by the saturation vapor pressure deficit (VPD), thus they seek a relative variable such as the relative humidity (RH) that is sensitive to VPD, therefore fSM was parametrized as $RH^{VPD/\beta}$, with β defining the relative sensitivity to VPD. Then the authors defined the relative extractable water as a normalized SM ratio. Liu (2022) developed different non-linear functions for simulating ET through ETpot constrained by SM at a daily scale. The ET simulation using non-linear functions resulted in higher accuracy than that of linear relations and CR methods.

Most of the abovementioned F parameterization did not consider the influence of atmospheric variables. Nevertheless, diverse authors such as Fisher *et al.* (2008), Zscheischler *et al.* (2015), Bagley *et al.* (2017), and Short Gianotti *et al.* (2019) highlighted the importance of the atmospheric variables on F variability and suggested that atmospheric parameterization should be incorporated in F estimation. So, atmospheric parameters, coupled with land explanatory variables, could reduce the F function's errors and produce more precise ET estimations.

Therefore, the current study aims to improve the accuracy of the ETsm and ETwv estimations by enhancing the F expression. In this sense, we propose to derive an F expression, i.e. the ET/ETpot ratio, applicable to different land covers, that incorporates land surface and atmospheric variables. The derived analytical F function will be included in ETsm and ETwv expressions and contrasted with ground-observed monthly mean daily ET measurements to evaluate their impact on the accuracy of ET estimations. Moreover, the resulting F expression will be coded in the Google Earth Engine (GEE) platform to generate ET maps.

2. Materials and methods

2.1. Review of ETsm and ETwv models

Walker *et al.* (2019a) published an expression to estimate ET (ETsm) based on Komatsu's results (Komatsu, 2003). He experimentally demonstrated that F would be directly linked to the surface wetness condition. However, the ET resistances are important limiting factors to estimate F at large scales using Komatsu's formulation. In this sense, Walker *et al.* (2019a) modified Komatsu's F expression by introducing SMsat and a calibration parameter X to avoid ET resistance coefficients estimation. So, the ratio ET/ETpot mainly depends on the SM and the soil type properties.

The ET calculation at the regional scale is formulated using Bouchet's CR (Bouchet, 1963), P-T equation, and the modified Komatsu's F concept;

$$\mathrm{ETsm} = \left(\frac{2\mathrm{F}}{\mathrm{F}+1}\right)\left[\alpha\left(\frac{\Delta}{\Delta+\gamma}\right)(\mathrm{NR}-\mathrm{G})\right], \mathrm{F} = 1-\exp\left(\frac{-\mathrm{SM}}{-\mathrm{SMsat}/\ln(1-\mathrm{X})}\right) \quad (1)$$

where SM is the soil moisture of any surface, SMsat is the soil moisture of the saturated surface, X is a calibration factor, α is the P-T parameter typically assumed 1.26, γ is the psychrometric constant, Δ is the slope of the saturation vapor pressure curve, F the relative evapotranspiration coefficient, Rn is the net radiation and G the surface soil heat flux.

Despite the precise ET results obtained, the ETsm model is limited to apply at those sites with ground observed data to calibrate the X parameter (see Walker *et al.*, 2019a).

Afterward, Walker *et al.* (2019b) presented an F formulation (named Fr) improving the relative evapotranspiration introduced by Venturini *et al.* (2008). As in Venturini *et al.* (2008), the assumption that the wind function similarly affects actual and potential ET was also used in Walker *et al.* (2019b). However, the authors proposed to estimate the surface actual water vapour pressure using surface texture information and SM content. As a result, the ratio SM/SMsat replaced the original Venturini *et al.*'s (2008) F formulation, in agreement with the ET-driven physical process. Thus, combining the modified F parameterization (Fr), P-T equation, and Granger's CR (Granger, 1989), the ETwv model was derived as follows;

$$\mathrm{ETwv} = \alpha\left(\frac{\mathrm{Fr}\,\Delta}{\mathrm{Fr}\Delta+\gamma}\right)(\mathrm{NR}-\mathrm{G}), \mathrm{Fr} = \frac{\mathrm{SM}}{\mathrm{SMsat}} \quad (2)$$

where SM is the soil moisture content, SMsat is the soil moisture of the saturated surface, α is the P-T parameter, γ is the psychrometric constant, Δ is the slope of the saturation vapor pressure curve, Fr is the relative evapotranspiration coefficient, Rn is the net radiation and G the surface soil heat flux.

Consequently, the derivate ETwv model is based on universal relationships, without calibration parameters and therefore, it is suitable to different data sources and to any remote region. The proposed ETsm and ETwv formulations extend the P-T equation to different surface wetness conditions, assuming that surface moisture and the available radiation energy are the driving factors in ET estimation. For further details see Walker *et al.* (2019a), and Walker *et al.* (2019b).

2.2. Proposed F methodology

Previous F formulations (Mintz and Walker, 1993; Komatsu, 2003; Detto *et al.*, 2006; An *et al.*, 2018; Liu, 2022), did not take into account the importance of atmospheric variables in the formulation. Considering Fisher *et al.* (2008), F can be explained by VPD, RH, and SM. Venturini *et al.* (2011) also suggested that F can be explained by the SM, SMsat, the air temperature (Ta), Rn, the slope of the saturation vapor pressure curve (Δ), RH, and the shortwave incoming radiation (SWin). In this analysis, the land surface properties are represented by SM and SMsat, the atmospheric conditions are characterized by Ta, Δ, and RH, and the available energy variables are summarized in Rn, G, and SWin.

Based on the nonlinearity of the F-SM relationship published by Mintz and Walker (1993), Orth *et al.* (2013), and Liu (2022), nonlinear functions were evaluated to estimate F with the SM, SMsat, Δ, Ta, Rn, RH, and SWin explanatory variables, specifically logarithmic and sigmoidal expressions were analysed. Liu (2022) demonstrated that the accuracy of the ET estimations using potential and exponential functions was higher than that of the linear regression method. In this sense, the logarithmic function is the inverse of the exponential function, with a general form of $Y=\log_b X$, where b is the logarithm base. Considering Komatsu's (2003) and Detto *et al.*'s (2006) results, the sigmoidal curve, which is a refined exponential model, was also tested in this work. The standard form for a sigmoid function, also known as a sigmoidal curve or logistic function, is $Y = \frac{1}{1+e^{-x}}$ (Von Seggern, 2007).

2.3. Model performance

To analyse the performance of the proposed functions the Root Mean Square Error (RMSE), bias, and determination coefficient (R^2), were quantified. The equations are:

$$\mathrm{RMSE} = \sqrt{\sum \frac{(\mathrm{ET_{obs}} - \mathrm{ET_{mod}})^2}{\mathrm{N}}} \quad (3)$$

$$\mathrm{Bias} = \sum \frac{(\mathrm{ET_{obs}} - \mathrm{ET_{mod}})}{\mathrm{N}} \quad (4)$$

$$\mathrm{R^2} = \frac{\sum(\mathrm{ET_{mod}} - \overline{\mathrm{ET}}_{\mathrm{obs}})^2}{\sum(\mathrm{ET_{obs}} - \overline{\mathrm{ET}}_{\mathrm{obs}})^2} \quad (5)$$

where N is the number of observations, ETobs is the *in situ* ET, ETmod is the modelled ET, and $\overline{\mathrm{ET}}_{\mathrm{obs}}$ is the mean value of ETobs.

2.4. Data

In this study, FLUXNET *in situ* observations and the SMsat map proposed by Walker and Venturini (2019) were used to derive F and estimate monthly mean daily ET.

The FLUXNET ground observations network consists of Eddy Covariance stations installed for quantifying carbon, water vapor, and energy fluxes (https://fluxnet.fluxdata.org/). Only the operative stations with high-quality SM and Latent Heat flux (LE) observations, i.e. with at least 60% of Rn reliable data and less than 2% of LE and SM outliers, were taken into consideration here (Purdy *et al.*, 2018; Walker and Venturini, 2019). In this preliminary analysis, 17 FLUXNET Eddy Covariance tower sites, distributed across the world were used. These stations are located in savanna (SAV), cropland (CRO), and forest (FOR) land covers. The site names, land use, and data set time span are listed in Table 1.

FLUXNET provides half-hour observations that were quality checked and averaged to obtain the monthly values of the variables used in this work, i.e. Ta (°C), Rn (W/m^2), Δ (Kpa/°C), SM (%), RH (%), SWin (W/m^2) and LE (W/m^2). These LE observations are then converted to ET using the latent heat of vaporization and the water density (Walker and Venturini, 2019).

The global SMsat map, published by Walker and Venturini (2019), was used to incorporate the soil properties spatial variability in F estimations. The soil texture classification provided by the Harmonized World Soil Database (HWSD) and Cosby *et al.* (1984) soil moisture saturation values were combined to create a layer of SMsat values, for each soil textural class. The SMsat layer has the original HWSD spatial resolution, of about 1 km (see Walker and Venturini, 2019).

3. Results and discussions

3.1. F estimation

Data from the 17 FLUXNET stations were processed without land cover discriminations,

Table 1. FLUXNET Eddy Covariance tower sites location, land cover, and time span of the data.

Country	Site	Latitude (°)	Longitude (°)	Land Cover	Time Span
Australia	AU-Cpr	-34.0021	140.5891	SAV	2010-2014
Australia	AU-DaS	-14.1593	131.3881	SAV	2008-2014
Australia	AU-Gin	-31.3764	115.7138	SAV	2011-2014
Australia	AU-How	-12.4943	131.1523	SAV	2001-2014
Australia	AU-Tum	-35.6566	148.1517	FOR	2001-2014
Belgium	BE-Lon	50.5516	4.7461	CRO	2004-2014
Belgium	BE-Vie	50.3050	5.9981	FOR	1996-2014
Germany	DE-Geb	51.1001	10.9143	CRO	2001-2014
Germany	DE-Kli	50.8931	13.5224	CRO	2004-2014
Germany	DE-Tha	50.9624	13.5652	FOR	1996-2014
French Guiana	GF-Guy	5.2788	-52.9249	FOR	2004-2014
Italy	IT-CA3	42.3800	12.0222	FOR	2011-2014
Italy	IT-Isp	45.8126	8.6336	FOR	2013-2014
Italy	IT-SR2	43.732	10.2910	FOR	2013-2014
USA	US-SRM	31.8214	-110.8661	SAV	2004-2014
USA	US-Ton	38.4316	-120.9660	SAV	2001-2018
USA	US-Tw3	38.1159	-121.6467	CRO	2013-2018

during the spring-summer growing time, since the warmer season is crucial for ET monitoring (Detto *et al.*, 2006, Li *et al.*, 2018). The individual contribution of the explanatory variables (SM, SMsat, Δ, Ta, Rn, RH, and SWin) on ET, was analysed by the r statistic. The highest correlation coefficient was found between ET and RH (r=0.60). The correlation between ET and Rn, Ta, Δ, and, SM variables showed r values of 0.33, 0.26, 0.24, and 0.21, respectively. On the other hand, SMsat and SWin presented low correlations with ET, i.e. 0.07 and -0.02 respectively. Hence, RH, SM, Rn, Ta, and Δ would make a significant contribution to explaining F variation.

As it was mentioned in Section 2.2, two nonlinear functions (logarithmic and sigmoid) were explored to derive F expressions that consider land surface and atmospheric variables. For this purpose, the ground observed data was partitioned into training and testing data sets. Thus, data from 13 FLUXNET Eddy Covariance towers were randomly selected for parameter tuning, and the data of the remaining four FLUXNET stations were used to verify and test the calibrated parameters. The selected explanatory variables, without further process, were used to fit the logarithmic function. To compute the sigmoid equation it was necessary to create a dependent variable (ω) that combines input variables. Given the large r statistic between RH and ET, RH was selected to integrate the dimensionless ω variable along with SM. Previous to ω calculation, SM was divided by SMsat and RH was normalized with the maximum and minimum values of the variable time series.

According to the least-squares method (Bretscher, 1995), the best-fitted curves are the following;

$$\mathrm{Fl} = \bar{\Delta} * \mathrm{Ln}\left(\frac{\mathrm{SM}}{\mathrm{SMsat}}\right) + \exp\left(\frac{-\overline{\mathrm{RH}}}{100}\right) \tag{6}$$

where $\bar{\Delta}$ is the mean slope of the saturation vapor pressure curve, SM is the soil moisture content, SMsat is the soil saturation water content, and $\overline{\mathrm{RH}}$ is the mean relative humidity.

$$\mathrm{Fs} = \frac{0{,}55}{1 + \exp\left(\frac{0.35 - \omega}{0.08}\right)} \tag{7}$$

where ω is the average between SM/SMsat ratio and the normalized RH. 0.55, 0.35, and 0.08 are calibrated parameters.

The proposed F parameterizations, i.e. Fl and Fs, consider the influence of atmospheric variables in the formulation as was suggested by Fisher *et al.* (2008), Zscheischler *et al.* (2015), Bagley *et al.* (2017), Short Gianotti *et al.* (2019), and Liu (2022). Figure 1 presents a boxplot diagram for the Fr, Fl, and Fs expressions evaluated here.

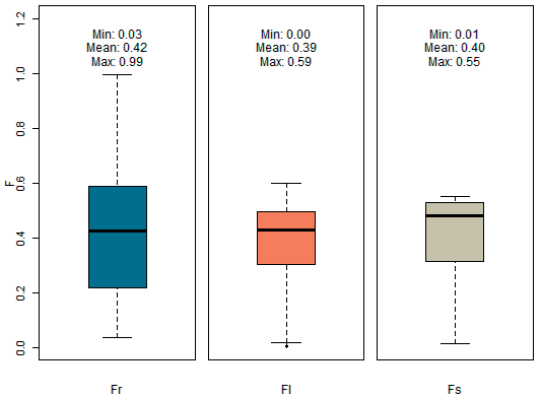

Figure 1. Boxplot diagram for each of the analysed F formulations, i.e. Fr, Fl, and Fs.

The Fr formulation, i.e. SM/SMsat, presented the largest dispersion of the data and achieved the highest maximum value (Max=0.99). The logarithmic and sigmoidal functions showed low maximum values (Fl=0.59 and Fs=0.55), differing from Fr in 0.40 and 0.44 respectively. All the F formulations yielded similar minimum and mean values. It can be observed that F variability is higher for Fr which only depends on the SM availability and it decreases if atmospheric variables are included in F parameterization. Thus, the following session analyses the errors of ET models with Fr, Fl and Fs.

3.2. ETsm and ETwv models performance evaluation

Six different formulations to estimate ET are obtained as a result of the combination of the evaluated F expressions (Fr, Fl, and Fs) with both ET models (ETsm and ETwv). Table 2 presents the resulting ET models and the name adopted for each of them.

Table 2. Nomenclature used to identify ET models. ETsm and ETwv are the Walker *et al.* (2019a) and Walker *et al.* (2019b) ET models, respectively. Fr, Fl, and Fs are the analysed F parameterizations.

	ET models	
F parameterizations	ETwv	ETsm
Fr	ETwvr	ETsmr
Fl	ETwvl	ETsml
Fs	ETwvs	ETsms

The performance of the six proposed ET models was evaluated. Monthly mean daily ET estimations obtained from the different methodologies were compared with monthly mean daily ET observations (ETobs) using the calibration data set. The data dispersion of each ET methodology *versus* ETobs is presented in Figure 2. The minimum, mean and maximum of ETobs and modelled ET are incorporated in this Figure.

The ETwv model presented a similar response to the three parameterizations, in contrast with ETsm that vary with each F equation. The Fl formulation combined with both ET models, i.e., ETsml and ETwvl, showed the lowest dispersion of the results and the highest number of outliers. On the other hand, the ET methods with Fr and Fs expressions (ETsmr, ETsms, ETwvr, and ETwvs) seem to reproduce the variability of the ETobs data.

The Fl formulation combined with ETwv and ETsm models showed the lowest minimum values, differing from the minimum ETobs in 0.71 mm/day and 0.63 mm/day, respectively. ETsm methodology yielded similar mean ET values than mean ETobs, with differences lower than 0.52 mm/day. The ETwv model shows higher maximum and mean values than ETobs.

Table 3 presents a summary of the R^2, RMSE, and bias for each evaluated methodology compared with *in situ* measurements. The ETwv and ETsm combined with Fs expression yielded the highest correlation with ETobs. The R^2 were 0.79 and 0.74 for ETwvs and ETsms, respectively. On the contrary, the lowest correlations were obtained using Fr parameterization in both ET models (ETwvr=0.59 and ETsmr=0.38). The ETsm and ETwv methodologies presented a lower error when Fs was incorporated into their formulation. The ETsms yielded a RMSE of 1.36 mm/day (22.8% in percentage of the mean ETobs) and ETwvs shows a RMSE of 1.45 mm/day (24.5% of the mean ETobs). The reader can observe that ETsms showed the lowest bias compared with the other models, and the ETwv method showed similar bias using all the proposed F parameterizations.

The contrast between ETobs and estimated ET from each proposed methodology is presented in Figure 3. It can be observed that ETsmr and ETwvr showed the highest dispersion around the 1:1 line. The ETwv methodology overestimated

Table 3. Determination coefficient (R^2), Root Mean Square Error (RMSE), and bias between monthly mean daily observed and estimated ET.

	ETwv			ETsm		
Statistic	ETwvr	ETwvl	ETwvs	ETsmr	ETsml	ETsms
R^2	0.59	0.63	**0.79**	0.38	0.57	**0.74**
RMSE (mm/day)	1.79	1.75	**1.45**	2.14	1.70	**1.36**
RMSE (%)	30.0	29.4	**24.5**	35.9	28.5	**22.8**
Bias (mm/day)	-0.76	-0.84	**-0.81**	0.51	0.48	**0.40**

Best statistics are highlighted in bold.

the ground ET measurements using the different F formulations. As was expected, ET estimates from ETsms and ETwvs models are closer to the 1:1 line than the other tested methodologies.

The model errors for each land cover class were estimated to verify their applicability at a regional scale. Thus, crop areas yield RMSE between 1.25 and 1.97 mm/day, being ETwvs the best model. In the case of savanna, the RMSE ranged from 1.45 mm/day (for ETsms) to 2.46 mm/day (for ETwvl). Finally, in forest areas, ETsms yield an error of 1.20 mm/day while ETsmr resulted in a RMSE of 2.12 mm/day.

The proposed ET methodologies and their calibrated parameters were verified using AU_Cpr, IT_Isp, Be_Lon, and IT_CA3 FLUXNET stations, over different land covers. Figure 4 presents the relationship between estimated and ETobs for this data set. The R^2, RMSE and bias metrics were added to the box of each methodology. It can be noted that the proposed ET models yielded the lowest RMSE in comparison with that obtained during the calibration. The accuracy of the ETsms and ETwvs methods outperformed the other tested methodologies. The RMSE were 1.24 and 1.23 mm/day for ETwvs and ETsms, respectively. All the formulations show high correlations with ETobs,

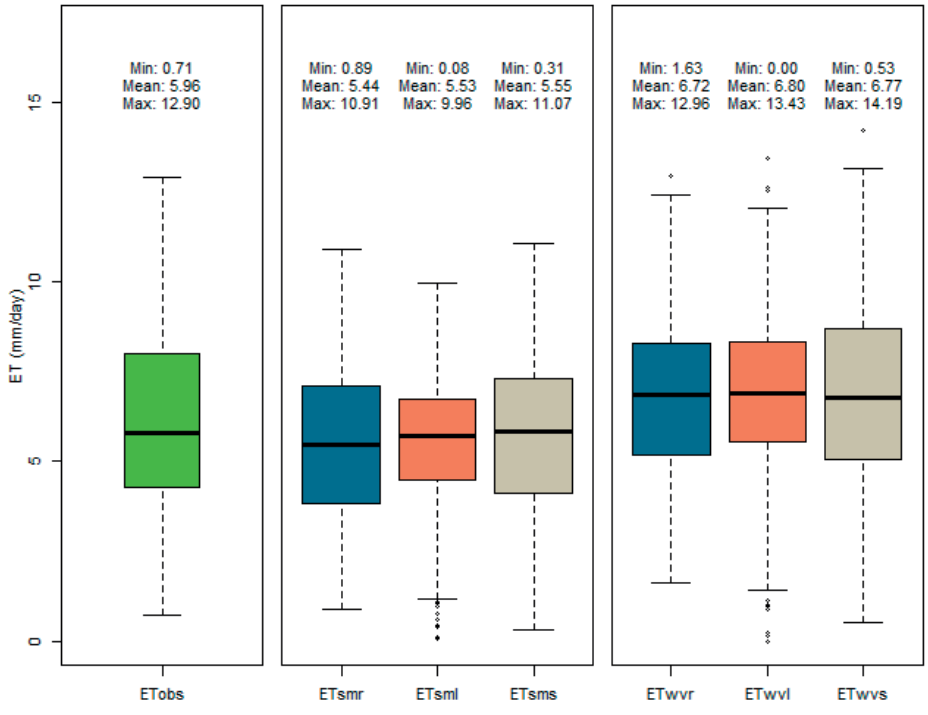

Figure 2. Boxplot diagram for each evaluated ET methodology (ETsmr, ETsml, ETsms, ETwvr, ETwvl, ETwvs) and observed ET (ETobs). Statistics minimum, mean, and maximum are included for monthly mean daily ETobs and estimated ET.

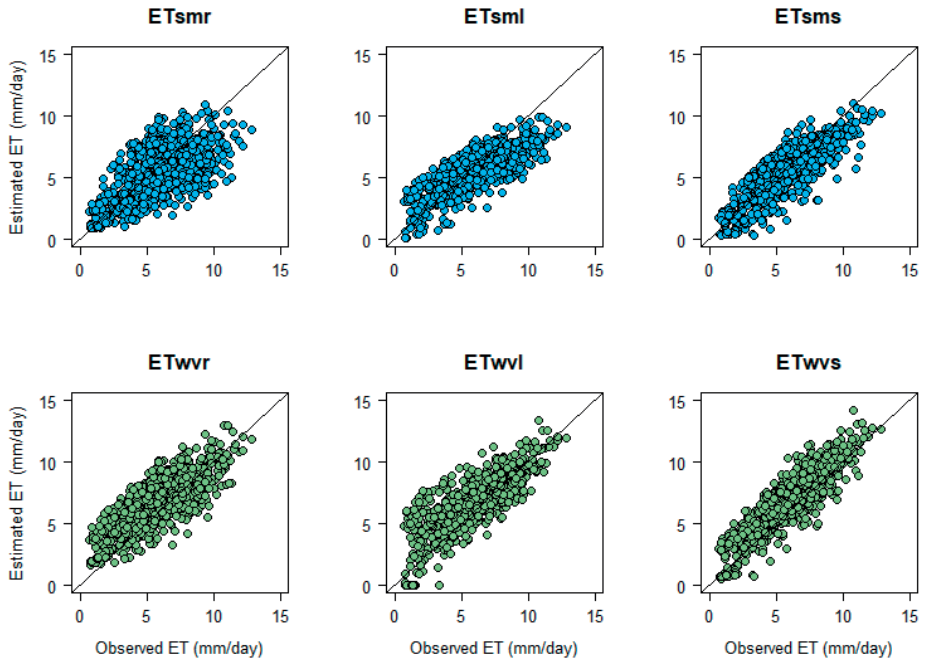

Figure 3. Relationship between monthly mean daily ETsmr, ETsml, ETsms, ETwvr, ETwvl, and ETwvs estimated ET and observed ET for the study period using the calibration data set. The solid black line represents the 1:1 line.

with R^2 higher than 0.66. The reader can observe that the ETwv method overestimated the *in situ* ET observations using the three F parameterizations. In contrast, the ETsm method yielded a moderate dispersion of the ET estimation.

In Figure 4 the AU_Cpr station in a SAV land cover displays the lowest ET values (see red points). The CRO site (BE_Lon) shows the intermediate ET values, coloured in green. As was expected, the highest ET values (orange and blue points) were achieved by the FOR sites IT_CA3 and IT_Isp.

The results presented show that Fs and Fl parameterizations surpassed Fr when they were incorporated into ETsm and ETwv methods, highlighting the importance of coupling driving variables in ET/ETpot models. Fisher *et al.* (2008) adjusted the soil evaporation using RH and VPD as a proxy of the SM content. They compared their result with FLUXNET observations, showing a strong correlation (R^2=0.90) with an RMSE of about 28% of the mean observed value. It is noteworthy that Fisher *et al.* (2008) final expression did not incorporate the surface properties and the proposed expression is complex. Brust *et al.* (2021) enhanced Terra Moderate Resolution Imaging Spectroradiometer (MODIS) ET model, (MOD16) using Soil Moisture Active Passive (SMAP) SM product. They compared their results with FLUXNET data and reported an RMSE of 30% of the mean observed ET. Liu (2022) applies a soil moisture index similar to that of Walker *et al.* (2019b) to constrain ETpot. He used different linear and nonlinear functions to estimate F and contrasted the result with FLUXNET observations, achieving RMSE of about 27% of the mean observed ET. The ET models proposed in this work coupled atmospheric and surface variables reducing the errors published by the aforementioned authors.

3.3. Application of the ET functions in Google Earth Engine

Passive microwave low frequencies (<5 GHz) are less sensitive to the vegetation biomass and the microwave emissions are more representative of the soil below to the surface (Entekhabi *et al.*, 2014). Thus, SMAP images are comparable to FLUXNET *in situ* observations, and the calibrated

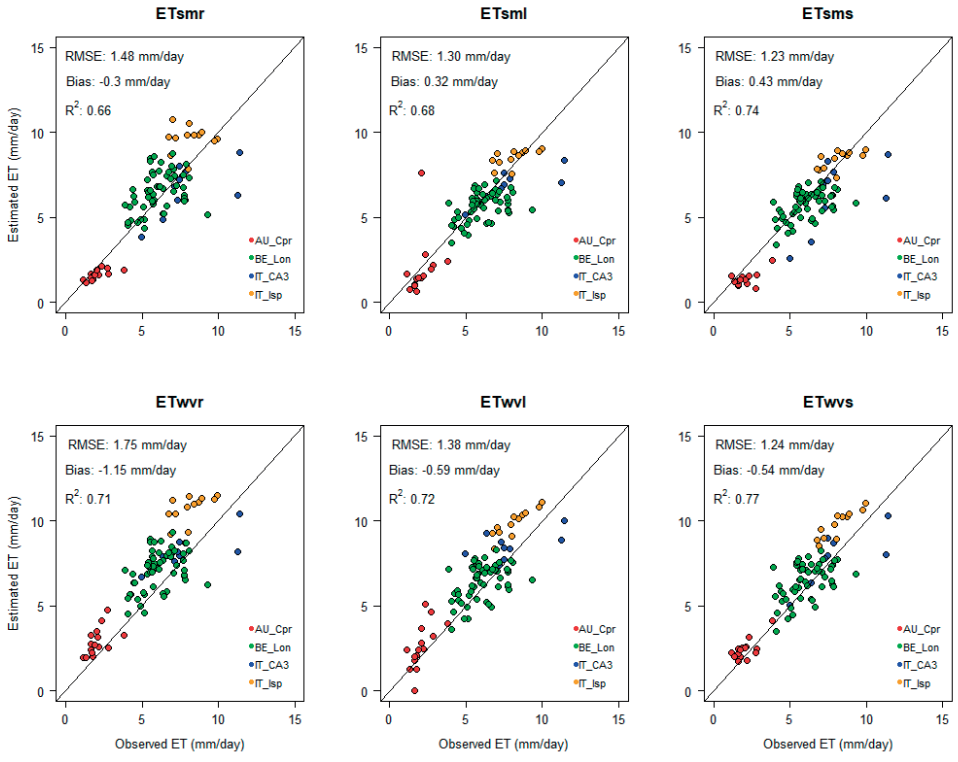

Figure 4. Relationship between monthly mean daily observed and estimated ETsmr, ETsml, ETsms, ETwvr, ETwvl, and ETwvs ET for verification purposes. The R^2, RMSE, and bias statistics are presented for each method. The validation sites are indicated in different colors; AU_Cpr (red), IT_CA3 (blue), BE_Lon (green), and IT_Isp (orange).

F functions can be applied with SMAP data. The ET models with the highest accuracy (ETsms and ETwvs) were coded in the GEE platform to obtain global ET maps. The Global Land Data Assimilation System Version 2.1 (GLDAS), SMAP dataset and the SMsat map (Walker and Venturini, 2019), were used. The GLDAS provides data from 2000 to the present, every eight hours at a global scale, with a spatial resolution of 0.25° (Rodell *et al.*, 2004). The SMAP mission carries a passive radiometer in L-band. It is orbiting since 2015, and it was devoted to provide global SM maps (Entekhabi *et al.*, 2014). In this study, the SPL3SMP_E.005 product has been used. This product provides SM data every 2-3 days with a spatial resolution of 9 km.

The operational global ET products Global Land-surface Evaporation Amsterdam Methodology (GLEAM) and MOD16 were used to compare with the proposed ETsms and ETwvs maps. GLEAM is a set of algorithms that estimate ET and their components based on satellite data and the P-T equation (Yang *et al.*, 2017). GLEAM v3.6b offers monthly aggregated ET maps at 0.25° spatial resolution spanning the period 2003-2021. The MOD16A2GF ET product is a 8-day composite dataset with a spatial resolution of 500m, covering the 2000-2022 time span. MOD16A2GF ET is the accumulation of 8-day total water loss (Mu *et al.* 2011). Here, GLEAM and MOD16 were converted to monthly mean daily ET and compared with the proposed ETsms and ETwvs maps.

ETwvs, ETsms, GLEAM, and MOD16 ET estimations were analysed for three sites distributed in different land covers during the 2015-2021 period, i.e., in a forest area in the Amazonia - Brazil (3°57’58’’ S, 65°37’42’’ W), in a cropland area in Rio Cuarto - Argentina (33°6’40’’ S, 64°12’58’’ W), and in Oklahoma - USA (36°36’18’’ N, 97°29’6’’ W) in a prairie. Figure 5 shows the temporal variation of the monthly mean daily ET estimations for the study

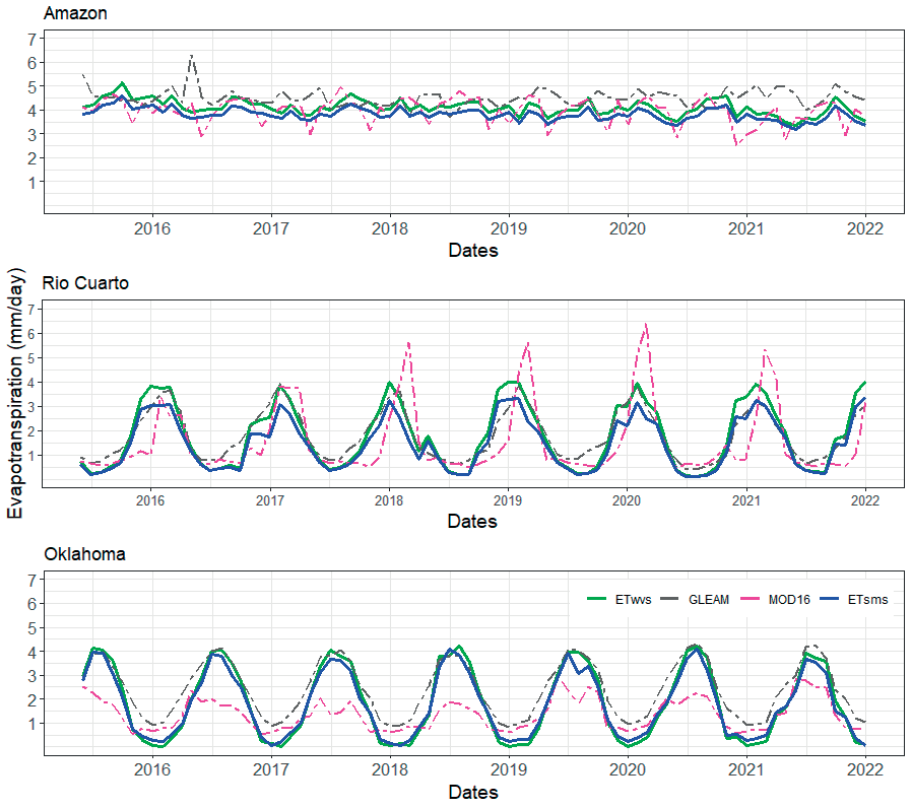

Figure 5. Monthly mean daily ETsms, ETwvs, GLEAM, and MOD16 ET estimations for a forest (Amazonia- Brazil), cropland (Río Cuarto- Argentina), and native prairie area (Oklahoma- USA) during the 2015-2021 period.

sites. In the Amazonia all the evaluated models show high ET estimations for the whole study period. For the cropland and native prairie sites the ET estimations achieve lower values, following an annual cycle. It can be observed that the proposed ETsms and ETwvs models produce similar ET estimations to GLEAM for the three land covers. MOD16 shows the lowest ET estimations for Amazonia and Oklahoma sites. Nevertheless, it achieves high values of ET in the cropland area. In this sense, different authors have demonstrated that GLEAM is a better product than MOD16 product in different land covers, compared with ground ET observations. Khan *et al.* (2018) evaluated GLEAM and MOD16 products with observed ET data in Asia. They suggested that MOD16 showed high errors over all vegetation conditions compared with GLEAM. Khan *et al.* (2020) published that GLEAM performed well in both forest and grassland biomes across Australia, although MOD16 tended to underestimate the flux tower measurements in all land cover types. More recently, Salazar-Martínez *et al.* (2022) analysed GLEAM and MOD16 products at low latitude eddy covariance sites. The authors concluded that in general GLEAM performs better than the MOD16 product. Similar results were published by Zhu *et al.* (2022) using observed data of a wide range of land cover types over all continents. The proposed ETsms and ETwvs models yield ET estimations comparable to the GLEAM data. Thus, it is possible to indicate that ETsms and ETwvs with GLDAS and SMAP produce reliable ET maps.

4. Conclusions

In this work, logarithmic and sigmoid relative evapotranspiration functions were proposed assuming that it depends on the surface properties and atmospheric variables. These two nonlinear functions were included in ETsm and ETwv models and contrasted with observed ET to

evaluate their impact on the accuracy of monthly mean daily ET results.

The calibrated Fl and Fs parameterizations presented were derived from observed SM data at point scale and extended to passive microwave sensor scale. This extension of the derived models reinforces the assumption that the first soil layer moisture can be integrated in the relative evapotranspiration index, consequently in ET models. However, it should be noted that monthly ET and coarse spatial resolutions are not entirely suitable to small agricultural practices. Although in this paper it was demonstrated that the proposed models yield good results for vulnerable forests monitoring (wildfire), regional water balances, climate change studies, and ecosystem evolution applications.

The derived ET models are flexible, so could be applicable to diverse combinations of dataset and to any remote region. In this sense, the proposed models improve the operational ET products at a global scale. The resulting ET maps are comparable to GLEAM maps for different land cover during the 2015-2021 period, being Fs and Fl scalable for many applications.

References

Allen, R., Morse, A., Tasumi, M., Bastiaanssen, W., Kramber, W., Anderson, H. 2001. Evapotranspiration from Landsat (SEBAL) for water rights management and compliance with multi-state water compacts. In IGARSS 2001. Scanning the Present and Resolving the Future. *Proceedings. IEEE 2001 Int. Geoscience and Remote Sensing Symposium*.

An, N., Tang, C.S., Xu, S.K., Gong, X.P., Shi, B., Inyang, H.I. 2018. Effects of Soil Characteristics on Moisture Evaporation. *Eng. Geol*., *239*, 126–135. https://doi.org/10.1016/j.enggeo.2018.03.028

Bagley, J., Kueppers, L., Billesbach, D., Williams, I., Biraud, S.C., Torn, M.S. 2017. The Influence of Land Cover on Surface Energy Partitioning and Evaporative Fraction Regimes in the U.S. Southern Great Plains. *J. Geophys. Res., 122*, 5793–5807. https://doi.org/10.1002/2017JD026740

Bouchet, R.J. 1963 Évapotranspiration Réelle Et Potentielle Signification Climatique. *Int. Assoc. Sci. Hydrol*., *62*, 134–162.

Bretscher, O. 1995. *Linear Algebra With Applications*, third ed. Upper Saddle River, NJ: Prentice Hall.

Brust, C., Kimball, J.S., Maneta, M.P., Jencso, K., He, M., Reichle, R.H. 2021. Using SMAP Level-4 Soil Moisture to Constrain MOD16 Evapotranspiration over the Contiguous USA. *Remote Sens. Environ*., *255*, 112277. https://doi.org/10.1016/j.rse.2020.112277

Brutsaert, W.A. 2015. Generalized Complementary Principle with Physical Constraints for Land-Surface Evaporation Wilfried. *Water Resour. Res*., *51*, 8087–8093. https://doi.org/10.1002/2015WR017720

Cosby, B.J., Hornberger, G.M., Clapp, R.B., Ginn, T.R. 1984. A Statistical Exploration of the Relationships of Soil Moisture Characteristics to the Physical Properties of Soils. *Water Resour. Res., 20*, 682–690. https://doi.org/10.1029/WR020i006p00682

Detto, M., Montaldo, N., Albertson, J.D., Mancini, M., Katul, G. 2006. Soil Moisture and Vegetation Controls on Evapotranspiration in a Heterogeneous Mediterranean Ecosystem on Sardinia, Italy. *Water Resour. Res*., *42*, 1–16. https://doi.org/10.1029/2005WR004693

Entekhabi, D., Yueh, S., O'Neill, P.E., Kellog, K.H., Allen, A., Bindlish, R., Das, N., *et al.* 2014. SMAP Handbook-Soil Moisture Active Passive: Mapping Soil Moisture and Freeze/Thaw from Space. National Aeronautic Space Administration.

Fisher, J.B., Tu, K.P., Baldocchi, D.D. 2008. Global Estimates of the Land-Atmosphere Water Flux Based on Monthly AVHRR and ISLSCP-II Data, Validated at 16 FLUXNET Sites. *Remote Sens. Environ*., *112*, 901–919. https://doi.org/10.1016/j.rse.2007.06.025

Fisher, J.B., Melton, F., Middleton, E., Hain, C., Anderson, M., Allen, R.,... Wood, E.F. (2017). The future of evapotranspiration: Global requirements for ecosystem functioning, carbon and climate feedbacks, agricultural management, and water resources. *Water resources research*, *53*(4), 2618–2626. https://doi.org/10.1002/2016WR020175

Granger, R.J. 1989. A Complementary Relationship Approach for Evaporation from Nonsaturated Surfaces. *J. Hydrol*., *111*, 31–38. https://doi.org/10.1016/0022-1694(89)90250-3

Khan, M., Liaqat, U., Baik, J., Choi, M. (2018). Stand-alone uncertainty characterization of GLEAM, GLDAS and MOD16 evapotranspiration products using an extended triple collocation approach. Agricultural and Forest Meteorology, *252*, 256–268. https://doi.org/10.1016/j.agrformet.2018.01.022

Khan, S.M., Baik, J., Choi, M. 2020. Inter-Comparison of Evapotranspiration Datasets over Heterogeneous Landscapes across Australia. *Adv. Sp. Res*., *66*, 533–545. https://doi.org/10.1016/j.asr.2020.04.037

Komatsu, T.S. 2003. Toward a Robust Phenomenological Expression of Evaporation Efficiency for Unsaturated Soil Surfaces. *J. Appl. Meteorol*., *42*, 1330–1334. https://doi.org/10.1175/1520-0450(2003)042%3C1330:TARPEO%3E2.0.CO;2

Laipelt, L., Kayser, R., Fleischmann, A., Ruhoff, A., Bastiaanssen, W., Erickson, T. Melton, F. (2021). Long-term monitoring of evapotranspiration using the SEBAL algorithm and Google Earth Engine cloud computing. *ISPRS Journal of Photogrammetry and Remote Sensing, 178*, 81–96. https://doi.org/10.1016/j.isprsjprs.2021.05.018

Li, Z., Li, Y., Bonsal, B., Manson, A.H., Scaff, L. 2018. Combined Impacts of ENSO and MJO on the 2015 Growing Season Drought on the Canadian Prairies. *Hydrol. Earth Syst. Sci*., *22*, 5057–5067. https://doi.org/10.5194/hess-22-5057-2018

Liu, J., You, Y., Li, J., Sitch, S., Gu, X., Nabel, J.E.,... Kong, D. (2021). Response of global land evapotranspiration to climate change, elevated CO2, and land use change. *Agricultural and Forest Meteorology*, *311*, 108663. https://doi.org/10.1016/j.agrformet.2021.108663

Liu, Z. 2022. Estimating Land Evapotranspiration from Potential Evapotranspiration Constrained by Soil Water at Daily Scale. *Sci. Total Environ*., *834*, 155327. https://doi.org/10.1016/j.scitotenv.2022.155327

Ma, N., Szilagyi, J., Jozsa, J. 2020. Benchmarking Large-Scale Evapotranspiration Estimates: A Perspective from a Calibration-Free Complementary Relationship Approach and FLUXCOM. J. *Hydrol*., *590*. https://doi.org/10.1016/j.jhydrol.2020.125221

Mintz, Y., Walker, G.K. 1993. Global Fields of Soil Moisture and Land Surface Evapotranspiration Derived from Observed Precipitation and Surface Air Temperature. *J. Appl. Meteorol*., *32*, 1305–1334. https://doi.org/10.1175/1520-0450(1993)032%3C1305:GFOSMA%3E2.0.CO;2

Mu, Q., Zhao, M., Running, S.W. 2011. Improvements to a MODIS global terrestrial evapotranspiration algorithm. *Remote Sens. Environ*., *115*, 1781–1800. https://doi.org/10.1016/j.rse.2011.02.019

Orth, R., Koster, R.D., Seneviratne, S.I. 2013. Inferring Soil Moisture Memory from Streamflow Observations Using a Simple Water Balance Model. *J. Hydrometeorol*., *14*, 1773–1790. https://doi.org/10.1175/JHM-D-12-099.1

Poulos, H., Barton, A., Koch, G., Kolb, T., Thode, A. 2021. Wildfire severity and vegetation recovery drive post-fire evapotranspiration in a southwestern pine-oak forest, Arizona, USA. *Remote Sens in Ecology and Conservation*, *7*(4), 579–591. https://doi.org/10.1002/rse2.210

Purdy, A.J., Fisher, J.B., Goulden, M.L., Colliander, A., Halverson, G., Tu, K., Famiglietti, J.S. 2018. SMAP Soil Moisture Improves Global Evapotranspiration. *Remote Sens. Environ*., *219*, 1–14. https://doi.org/10.1016/j.rse.2018.09.023

Rodell, M., Houser, P.R., Jambor, U., Gottschalck, J., Mitchell, K., Meng, C.-J., Arsenault, K., Cosgrove, B., Radakovich, J., Bosilovich, M., *et al.* 2004. The Global Land Data Assimilation System. Bull. *Am. Meteorol. Soc*., *85*, 381–394. https://doi.org/10.1175/BAMS-85-3-381

Salazar-Martínez, D., Holwerda, F., Holmes, T., Yépez, E.A., Hain, C.R., Alvarado-Barrientos, S., Vivoni, E. 2022. Evaluation of remote sensing-based evapotranspiration products at low-latitude eddy covariance sites. *Journal of Hydrology, 610*, 127786. https://doi.org/10.1016/j.jhydrol.2022.127786

Short Gianotti, D., Rigden, A., Salvucci, G., Entekhabi, D. 2019. Satellite and Station Observations Demonstrate Water Availability's Effect on Continental-Scale Evaporative and Photosynthetic Land Surface Dynamics. *Water Resour. Res*., 55, 540–554. https://doi.org/10.1029/2018WR023726

Sun, Z., Wei, B., Su, W., Shen, W., Wang, C., You, D., Liu, Z. (2011). Evapotranspiration estimation based on the SEBAL model in the Nansi Lake Wetland of China. *Mathematical and Computer Modelling, 54*(3-4), 1086–1092. https://doi.org/10.1016/j.mcm.2010.11.039

Teng, J., Yasufuku, N., Liu, Q., Liu, S. 2014. Experimental Evaluation and Parameterization of Evaporation from Soil Surface. *Nat. Hazards*, *73*, 1405–1418. https://doi.org/10.1007/s11069-014-1138-z

Venturini, V., Islam, S., Rodriguez, L. 2008. Estimation of Evaporative Fraction and Evapotranspiration from MODIS Products Using a Complementary Based Model. *Remote Sens. Environ*., *112*, 132–141. https://doi.org/10.1016/j.rse.2007.04.014

Venturini, V., Rodriguez, L., Bisht, G. 2011. A Comparison among Different Modified Priestley and Taylor Equations to Calculate Actual Evapotranspiration with MODIS Data. *Int. J. Remote Sens*., *32*, 1319–1338. https://doi.org/10.1080/01431160903547965

Von Seggern, D.H, 2007. CRC standard curves and surfaces with mathematica, second ed. CRC Press.

Walker, E., García, G.A., Venturini, V. 2019a. Evapotranspiration Estimation Using SMAP Soil Moisture Products and Bouchet Complementary Evapotranspiration over Southern Great Plains. *J. Arid Environ*., *163*, 34–40. https://doi.org/10.1016/j.jaridenv.2019.01.002

Walker, E., García, G.A., Venturini, V., Carrasco, A. 2019b. Regional Evapotranspiration Estimates Using the Relative Soil Moisture Ratio Derived from SMAP Products. *Agric. Water Manag*., *216*, 254–263. https://doi.org/10.1016/j.agwat.2019.02.009

Walker, E., Venturini, V. 2019. Land Surface Evapotranspiration Estimation Combining Soil Texture Information and Global Reanalysis Datasets in Google Earth Engine. *Remote Sens. Lett*., *10*, 929–938. https://doi.org/10.1080/2150704X.2019.1633487

Yang, X., Yong, B., Ren, L., Zhang, Y., Long, D. 2017. Multi-Scale Validation of GLEAM Evapotranspiration Products over China via ChinaFLUX ET Measurements. *Int. J. Remote Sens*., *38*, 5688–5709. https://doi.org/10.1080/01431161.2017.1346400

Yao, Y., Liao, X., Xiao, J., He, Q., Shi, W. 2023. The Sensitivity of Maize Evapotranspiration to Vapor Pressure Deficit and Soil Moisture with Lagged Effects under Extreme Drought in Southwest China. *Agric. Water Manag., 277*, 108101. https://doi.org/10.1016/j.agwat.2022.108101

Yunfei, L., Dongwei, G., Changjun, Y., Lei, Z., Dongping, X., Yi, L., Fanjiang, Z., Ahmed, Z., Xiaoping, C. 2023. Estimating the Temporal and Spatial Variations in Evapotranspiration with a Nonlinear Evaporation Complementary Relationship Model in Hyper-Arid Areas. *Water Resour. Manag., 37*, 521–535. https://doi.org/10.1007/s11269-022-03384-x

Zhou, S., Williams, A., Lintner, B., Berg, A., Zhang, Y., Keenan, T., Cook, B., Hagemann, S., Seneviratne, S., Gentine, P. 2021. Soil Moisture–Atmosphere Feedbacks Mitigate Declining Water Availability in Drylands. *Nat. Clim. Chang*., *11*, 38–44. https://doi.org/10.1038/s41558-020-00945-z

Zhu, W., Tian, S., Wei, J., Jia, S., Song, Z. (2022). Multi-scale evaluation of global evapotranspiration products derived from remote sensing images: Accuracy and uncertainty. *Journal of Hydrology, 611*, 127982. https://doi.org/10.1016/j.jhydrol.2022.127982

Zscheischler, J., Orth, R., Seneviratne, S.I. 2015. A Sub-Monthly Database for Detecting Changes in Vegetation-Atmosphere Coupling. *Geophys. Res. Lett*., *42*, 9816–9824. https://doi.org/10.1002/2015GL066563